Carpal Tunnel Morphological Modeling Using Ultrasound Imaging Validated by MRI

[1]Mary N. Henderson, [1]David Jordan, [1,2,3]Zong-Ming Li
[1]Hand Research Laboratory, Department of Orthopaedic Surgery, University of Arizona, Tucson, Arizona; [2]Department of Biomedical Engineering, University of Arizona, Tucson, Arizona; [3]University of Arizona Arthritis Center, Tucson, Arizona
Email: lizongming@arizona.edu

Disclosures: Henderson (N), Jordan (N), Li (N)

INTRODUCTION: There are an abundance of soft tissues surrounding the carpal tunnel, making it difficult to estimate an accurate carpal tunnel boundary based on bone boundaries, using common in-vivo imaging techniques [1]. Magnetic resonance imaging (MRI) and computed tomography (CT) have been used to view morphological properties in vivo and to visualize the carpal tunnel boundary [2,3]. However, these modalities are not ideal for routine point of care use due to the high costs and long imaging time, and in the case of CT imaging, radiation exposure is involved. Ultrasound imaging offers a more conveniently available method for imaging the carpal tunnel contents, but lacks the ability to view the carpal tunnel boney boundary provided by MRI and CT. The purpose of this study was to develop a model to estimate the area and shape of the carpal tunnel from ultrasound images validated by MRI.

METHODS: Six fresh frozen female cadaver hands were used for this study (age = 56.3 ± 6.7 years, BMI = 24.0 ± 7.6 kg/m^2). Each specimen was secured supine in a custom splint. An ultrasound probe was transversely positioned at the wrist to image the distal carpal tunnel, including the hook of hamate (HH), volar surface of capitate (CP), volar surface of the trapezoid (TP), ridge of the trapezium (TRP) and the thenar muscle ulnar attachment point to the transverse carpal ligament (TUP) (Figure 1a). A 7 Tesla MRI machine with an 84 mm-diameter coil was used to image each specimen. A scanning plane parallel to the transverse cross-section of the distal carpal tunnel was applied and 2D TE 8ms MRI images were taken. A single slice of the MRI scan containing the HH and TRP was selected for analysis. A custom MATLAB script was written to analyze the images. The MRI carpal tunnel boundary and bone boundary were manually traced (Figure 1b). The cartesian coordinates (x, y) of each point on the traced boundaries were converted to polar coordinates (r, θ). θ = 0° was defined at the TUP. The difference between the r values for the bone boundary r_{bone} and tunnel boundary r_{tunnel} were calculated at every 1° up to 360° and converted to percentages relative to r_{bone}, $r_{percent}$. 11 feature points were identified on each carpal bone, including 3 on the radial surface of the hamate, 2 on the volar surface of the capitate, 2 on the volar surface of the trapezoid and 4 on the ulnar surface of the trapezium. Vector distances from these landmarks were calculated from the HH, CP, TP and TRP, respectively, and transformed into an anatomical coordinate system defined by an origin at HH, x-axis in the direction from HH to TRP and y-axis perpendicular to the x-axis dorsally. For the ultrasound prediction, the visible landmarks of HH, CP, TP, TRP and TUP were manually identified. Leave-one-out analysis was used to first predict the location of the 11 feature points based on the average location vectors of these points, calculated from the remaining specimens. The bone boundary was spline fitted through the predicted points. The ultrasound bone boundary was converted to polar coordinates. The r values of the ultrasound bone boundary were adjusted at every 1° by multiplying by the average $r_{percent}$ for the remaining five specimens, giving the predicted ultrasound tunnel boundary. For each specimen, the area and circularity ($4\pi * \text{area}/\text{perimeter}^2$) of the MRI and ultrasound tunnel boundaries were calculated. Paired t-tests were used to compare MRI and ultrasound tunnel area and circularity ($\alpha = 0.05$).

RESULTS: Figure 2 shows the carpal tunnel boundaries from an MRI and ultrasound image, superimposed for comparison. In this example, the shapes align closely from the thenar muscle ulnar attachment point to the hook of hamate. However, there is a deviation in the region from the dorsal aspect of the hamate bone to the ridge of trapezium. The MRI and predicted ultrasound tunnel area were 132.8 ± 24.8 mm^2 and 134.9 ± 24.8 mm^2. There were no significant differences between the MRI area and ultrasound area ($p = 0.765$) with mean value of 2.1 mm^2 (95% CI: -14.8 to 18.9 mm^2). There was no significant difference ($p = 0.167$) between the circularity of MRI-based (0.78 ± 0.04) shape and that based on ultrasound prediction (0.74 ± 0.06).

DISCUSSION: A model was developed for predicting the carpal tunnel boundary using ultrasound and was validated by MRI. The estimated ultrasound areas were slightly larger compared to the MRI areas, indicating minor deviation in the reconstructed tunnel boundary based on the selected feature points. A previous study recognized the variation in carpal tunnel structure, specifically the positions of the carpal bones and soft tissue [4]. The limited sample size may have influenced the capability of our model in accounting for such variations. Similar studies estimating tunnel boundary used an automated MRI segmentation model based off soft tissue landmarks and, when compared to manually traced boundaries, also showed slight differences in boundary contours [5]. In the current study, the low difference between MRI and ultrasound area and between MRI and ultrasound circularity demonstrates the efficacy of our model in predicting the carpal tunnel boundary. Future work will include in-vivo analysis using a larger sample size to increase the accuracy of the predictive model.

SIGNIFICANCE/CLINICAL RELEVANCE: This model is a first step in estimating the carpal tunnel boundary from ultrasound images, which can serve as a quick and non-invasive method for obtaining an accurate carpal tunnel area and shape for point of care use.

REFERENCES: [1] Gabra and Li, J Wrist Surg, 2, 73–78, 2013. [2] Bleekman et al., Neurol, 35, 1599–1604, 1985. [3] Merhar et al., Skel Radiol, 15, 549–552, 1986. [4] Jordan et al., IET, 12, 2550009, 2025. [5] Chen et al., J Digit Imaging, 26, 510–520, 2013.

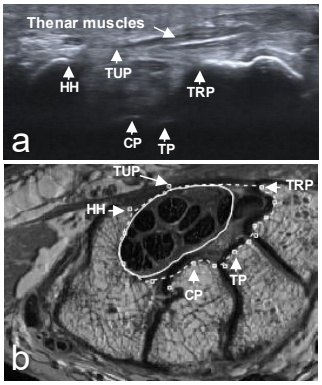

Figure 1. Ultrasound and MRI imaging. An ultrasound image with bone landmarks HH, CP, TP and TRP (a), and an MRI slice showing bone landmarks, bone boundary and carpal tunnel boundary (b), were taken of each specimen.

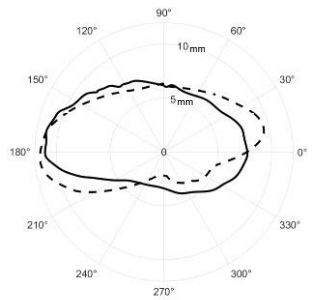

Figure 2. An example of carpal tunnel boundaries of MRI (solid) and ultrasound (dotted) on a polar plot

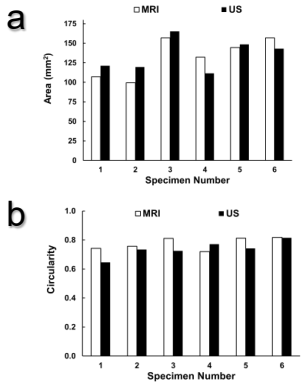

Figure 3. Carpal tunnel area (a) and circularity(b) based on MRI and US.